
CZECH TECHNICAL UNIVERSITY
Faculty of Nuclear Sciences and Physical
Engineering

Propositions of a thesis:

Mathematical Modelling and Numerical
Solution of Some 2D- and 3D-cases of
Atmospheric Boundary Layer Flow

Ing. Ivo Sládek

2005

Dizertační práce byla vypracována v rámci doktorského studia na Katedře matematiky Fakulty jaderné a fyzikálně inženýrské ČVUT v Praze.

Uchazeč: Ing. Ivo Sládek

Obor studia: Matematické modelování

Školitel: Prof. RNDr. Karel Kozel, DrSc.
Ústav technické matematiky,
U201, FSI ČVUT, Karlovo nám. 13, 121 35, Praha

Oponenti:
Doc. Ing. Richard Liska, CSc.
FJFI ČVUT, Brehova 7, 115 19, Praha 1

Doc. Ing. Jaroslav Fořt, CSc.
Ústav technické matematiky,
U201, FSI ČVUT, Karlovo nám. 13, 121 35, Praha 2

Doc. RNDr. Josef Brechler, CSc.
Katedra meteorologie a ochrany prostředí,
MFF UK, V Holešovičkách 2, 180 00, Praha 8

Teze byly rozeslány dne:

Obhajoba dizertace se koná dne: v hod.
před komisí pro obhajobu dizertační práce ve studijním oboru Matematické modelování Fakulty jaderné a fyzikálně inženýrské ČVUT v Praze.

S dizertací je možno se seznámit na děkanátě Fakulty jaderné a fyzikálně inženýrské ČVUT v Praze, na oddělení pro vědeckou a výzkumnou činnost, Břehová 7, Praha.

.....
Předseda

Obsah

1	Objectives of the work	5
2	Mathematical model	6
2.1	RANS system with algebraic turbulence model – (S1) .	6
2.2	RANS system with $k - \varepsilon$ turbulence model – (S2) . . .	7
2.3	Boundary conditions	8
3	Numerical method	11
3.1	The artificial compressibility method	11
3.2	Numerical treatment of the (S1), (S2)–systems	11
3.3	Time integration method	14
3.4	The artificial diffusion	15
4	Validation	16
5	Applications	19
6	Summary	22

1 Objectives of the work

The main goals of this work can be summarized in the following few points, the red ones are the major ones:

- 1) **Definition of mathematical model** – counting a set of partial differential equations general enough to describe the ABL flow
- 2) **Definition of turbulence model** one of the most important part of this work since two different models have been described in detail then validated and compared
- 3) **Definition of boundary conditions** – for all computed quantities, depending on the choice of turbulence model and the way of integration of equations, either to a solid wall or using a wall-function concept. One of the presented real-case problem is devoted to both wall modelling approaches.
- 4) **Definition of suitable numerical method** – accurate enough and easy to implement
- 5) **Validation of the models** – one of the key practical part of this work since it gives an idea about the degree of a credibility of the mathematical model to represent the real world
- 6) **Application of the model to a real-case ABL problems** – a number of practical real-case 2D and 3D problems have been defined and evaluated and some of them compared with the other numerical results by the other author as well.

2 Mathematical model

The atmospheric boundary layer flow in our case is supposed to be viscous, turbulent, stratified in general and moreover it can be approximated by the incompressible fluid Jaňour (2001) [1]. Hence the unknown variables to be determined are: the pressure p , the velocity vector $\vec{v} = (u, v, w)^T$ and the potential temperature Θ . In order to account for a pollution dispersion, one has to add the transport equation for the concentration C as well.

The system of governing equations is based on the full Reynolds averaged Navier–Stokes equations (RANS) written in the conservative form. The closure of the problem is performed by either a simple algebraic turbulence model or a more sophisticated two–equation $k - \varepsilon$ turbulence model as follows.

2.1 RANS system with algebraic turbulence model – (S1)

The system includes the continuity equation, the momentum equations and the transport equations for the concentration of passive pollutant and for the potential temperature, Jaňour (2001) [1]. The vector form is

$$\vec{F}_x + \vec{G}_y + \vec{H}_z = \vec{R}_x + \vec{S}_y + \vec{T}_z + \vec{f} \quad (1)$$

where \vec{F} , \vec{G} , \vec{H} represent the inviscid fluxes, \vec{R} , \vec{S} , \vec{T} abbreviate the viscous ones and \vec{f} denotes the vector of volume forces

$$\begin{aligned} \vec{F} &= \left(u, u^2 + \frac{p}{\rho}, uv, uw, Cu, \Theta u \right)^T, \\ \vec{G} &= \left(v, vu, v^2 + \frac{p}{\rho}, vw, Cv, \Theta v \right)^T, \\ \vec{H} &= \left(w, wu, wv, w^2 + \frac{p}{\rho}, Cw, \Theta w \right)^T, \\ \vec{R} &= \left(0, Ku_x, Kv_x, Kw_x, K^{(C)}C_x, K^{(\Theta)}\Theta_x \right)^T, \\ \vec{S} &= \left(0, Ku_y, Kv_y, Kw_y, K^{(C)}C_y, K^{(\Theta)}\Theta_y \right)^T, \\ \vec{T} &= \left(0, Ku_z, Kv_z, Kw_z, K^{(C)}C_z, K^{(\Theta)}\Theta_z \right)^T, \\ \vec{f} &= \left(0, fv, -fu, -g, 0, 0 \right)^T \end{aligned} \quad (2)$$

and the turbulent diffusion coefficients are computed from

$$K = \nu + \nu_T, \quad K^{(C)} = \frac{D}{\rho} + \frac{\nu_T}{\sigma_C}, \quad K^{(\Theta)} = \frac{k}{\rho c_p} + \frac{\nu_T}{\sigma_\Theta} \quad (3)$$

where σ_C , σ_Θ denote the turbulent Prandtl's numbers and the turbulent viscosity ν_T is given by

$$\nu_T = l^2 \left[\left(\frac{\partial u}{\partial z} \right)^2 + \left(\frac{\partial v}{\partial z} \right)^2 \right]^{1/2} \quad (4)$$

where l denotes the mixing length and due to Blackadar (1962) [2] we have

$$l = \frac{\kappa(z + z_0)}{1 + \frac{\kappa(z+z_0)}{l_\infty}} \quad (5)$$

where $\kappa \in < 0.36, 0.41 >$ is the von Karman constant and z_0 denotes the roughness parameter, l_∞ refers to the mixing length in the free atmosphere.

2.2 RANS system with $k - \varepsilon$ turbulence model – (S2)

Two additional transport equations for the turbulent kinetic energy (t.k.e.) and the rate of dissipation of the t.k.e. have to be incorporated into the system (S1) where the potential temperature equation is dropped out since this model is suitable for the indifferent atmospheric stratification, Jaňour (2001) [1]. The vector form of system is

$$\vec{F}_x + \vec{G}_y + \vec{H}_z = \vec{R}_x + \vec{S}_y + \vec{T}_z + \vec{f} + \vec{q} \quad (6)$$

where notation is similar as in the above case concerning the vectorial form of the system (S1) apart \vec{q} which represents the source term vector

$$\begin{aligned} \vec{F} &= (u, u^2 + \frac{p}{\rho}, uv, uw, Cu, ku, \varepsilon u)^T, \\ \vec{G} &= (v, vu, v^2 + \frac{p}{\rho}, vw, Cv, kv, \varepsilon v)^T, \\ \vec{H} &= (w, wu, wv, w^2 + \frac{p}{\rho}, Cw, kw, \varepsilon w)^T, \\ \vec{R} &= (0, Ku_x, Kvx, Kw_x, K^{(C)}C_x, K^{(k)}k_x, K^{(\varepsilon)}\varepsilon_x)^T, \\ \vec{S} &= (0, Ku_y, Kvy, Kw_y, K^{(C)}C_y, K^{(k)}k_y, K^{(\varepsilon)}\varepsilon_y)^T, \end{aligned}$$

$$\begin{aligned}
\vec{T} &= (0, Ku_z, Kv_z, Kw_z, K^{(C)}C_z, K^{(k)}k_z, K^{(\varepsilon)}\varepsilon_z)^T, \\
\vec{f} &= (0, fv, -fu, 0, 0, 0, 0)^T, \\
\vec{q} &= (0, 0, 0, 0, 0, (P - \varepsilon), (C_{\varepsilon 1}f_1\frac{\varepsilon}{k}P - C_{\varepsilon 2}f_2\frac{\varepsilon^2}{k}))^T. \quad (7)
\end{aligned}$$

where the new turbulent diffusion coefficients read

$$K^{(k)} = \nu + \frac{\nu_T}{\sigma_k}, \quad (8)$$

$$K^{(\varepsilon)} = \nu + \frac{\nu_T}{\sigma_\varepsilon}. \quad (9)$$

The turbulent viscosity ν_T is given by

$$\nu_T = C_\mu f_\mu \frac{k^2}{\varepsilon}. \quad (10)$$

where the wall damping functions f_μ, f_1, f_2 are defined by the following relations, Speziale *et.al.* (1992) [3]

$$f_\mu = \left(1 + \frac{3.45}{\sqrt{\text{Re}_t}}\right) \left[1 - e^{(-\frac{z^+}{70})}\right], \quad (11)$$

$$f_1 = 1, \quad (12)$$

$$f_2 = \left[1 - e^{(-\frac{z^+}{4.9})}\right]^2 \quad (13)$$

where $\text{Re}_t = \frac{k^2}{\nu\varepsilon}$ and the model constants read

$$C_\mu = 0.09, \quad \sigma_k = 1.0, \quad \sigma_\varepsilon = 1.3, \quad C_{\varepsilon 1} = 1.44, \quad C_{\varepsilon 2} = 1.83. \quad (14)$$

2.3 Boundary conditions

Very important part of mathematical modelling is related to specification of boundary conditions, mainly close to a wall where we can distinguish a two different approaches:

- **integration directly to a wall:** the grid should be sufficiently fine in the wall-normal direction to resolve a steep gradients of the computed quantities.

– Velocity components: the no-slip condition

$$u = 0, \quad v = 0, \quad w = 0. \quad (15)$$

- Concentration: no sedimentation allowed

$$\frac{\partial C}{\partial z} = 0. \quad (16)$$

- Turbulent kinetic energy: viscous effects dominates close to a wall and t.k.e. is therefore dissipated

$$k = 0. \quad (17)$$

- Dissipation rate: usually one of the following two possibilities is used

$$\frac{\partial \varepsilon}{\partial z} = 0, \quad \nu \frac{\partial^2 k}{\partial z^2} = \varepsilon, \quad 2\nu \left(\frac{\partial \sqrt{k}}{\partial z} \right)^2 = \varepsilon. \quad (18)$$

- **use of a wall functions**: it bypasses the direct integration to a wall and instead of it the profiles of velocity, temperature and other quantities are obtained from an analytical expressions. Since the grid need not to be so fine in the wall vicinity the computational process is much faster, but there are some limitations like *e.g.* flow separation.

- Velocity magnitude U : in the case of indifferent stratification

$$\frac{U}{u_\tau} = \frac{1}{\kappa} \ln \left(\frac{z + z_0}{z_0} \right) \quad (19)$$

where z_0 is the roughness parameter, U denotes the velocity magnitude at wall–distance z and u_τ refers to the friction velocity.

- Concentration: no sedimentation allowed

$$\frac{\partial C}{\partial z} = 0. \quad (20)$$

- Turbulent kinetic energy: it is possible to derive

$$k = \frac{u_\tau^2}{\sqrt{C_\mu}}. \quad (21)$$

- Dissipation rate: it is possible to derive

$$\varepsilon = \frac{u_\tau^3}{\kappa(z_1 + z_0)}. \quad (22)$$

The integration of governing equations goes from particular level $z = z_1$ and above it. A typical value for z_1 is around 50 *m*. The computed profiles are then patched together with the analytical ones at the level $z = z_1$.

Remark

A realization of conditions for pressure next to solid wall is set to fulfill the following expression

$$\frac{\partial p}{\partial n} = 0 \tag{23}$$

that is consistent with the normal momentum equation at solid wall. Through the open boundary, the pressure is extrapolated which enables the pressure waves to leave the computational domain without reflection back.

3 Numerical method

3.1 The artificial compressibility method

The systems (S1) and (S2) describe the steady, viscous, incompressible, turbulent flow and they are modified by the *artificial compressibility method*. As a result, the continuity equation takes the form

$$\frac{1}{\beta^2} p_t + u_x + v_y + w_z = 0 \quad (24)$$

where the β parameter stands for the artificial sound speed. So now, we can rewrite the vector form of the both systems (S1) and (S2) as follows

$$\mathbf{P} \cdot \vec{W}_t + \vec{F}_x + \vec{G}_y + \vec{H}_z = \vec{R}_x + \vec{S}_y + \vec{T}_z + \vec{f} + \vec{q} \quad (25)$$

where the vector \vec{W} of unknown variables reads

$$\vec{W} = (p, u, v, w, C, \Theta)^T \quad \text{for the (S1)–system,} \quad (26)$$

$$\vec{W} = (p, u, v, w, C, k, \varepsilon)^T \quad \text{for the (S2)–system} \quad (27)$$

and the matrix \mathbf{P} looks

$$\mathbf{P} = \begin{pmatrix} \frac{1}{\beta^2} & 0 & \dots & 0 \\ 0 & 1 & \dots & 0 \\ \vdots & \vdots & \ddots & \vdots \\ 0 & 0 & \dots & 1 \end{pmatrix}. \quad (28)$$

Now, the unsteady system of equations (25) is solved under the stationary boundary conditions, for an artificial time $t \rightarrow \infty$ to obtain the expected steady–state solution of the given problem for all of the variables (26) or (27).

3.2 Numerical treatment of the (S1), (S2)–systems

The numerical method is on the basis of the finite volume method of cell–centered type, applied to the systems of governing equations (S1) or (S2), respectively.

The computational domain Ω is divided into the structured system of a hexahedral control cells Ω_{ijk} in each direction of the Cartesian coordinate system. This system of control cells forms the non–orthogonal finite volume mesh.

Both systems (S1), (S2) written in compact vector form (25) are integrated over each control cell Ω_{ijk}

$$\begin{aligned} \iiint_{\Omega_{ijk}} \mathbf{P} \cdot \vec{W}_t dV = & - \iiint_{\Omega_{ijk}} [(\vec{F} - \vec{R})_x + (\vec{G} - \vec{S})_y + (\vec{H} - \vec{T})_z] dV + \\ & + \iiint_{\Omega_{ijk}} (\vec{f} + \vec{q}) dV. \end{aligned} \quad (29)$$

Using the ‘‘Divergence theorem’’ and the ‘‘Mean value theorem’’ one can rewrite (29) to the form

$$\begin{aligned} \mathbf{P} \cdot \vec{W}_t|_{ijk} = & - \frac{1}{\mu_{ijk}} \oint_{\partial\Omega_{ijk}} [(\vec{F} - \vec{R}) dS_1 + (\vec{G} - \vec{S}) dS_2 + (\vec{H} - K\vec{T}) dS_3] + \\ & + (\vec{f} + \vec{q})|_{ijk} \end{aligned} \quad (30)$$

where $\vec{W}_t|_{ijk}$ is the mean value of \vec{W} over cell Ω_{ijk} , $(\vec{f} + \vec{q})|_{ijk}$ represents the mean value of the volume forces and the source term over cell Ω_{ijk} and $\mu_{ijk} = \iiint_{\Omega_{ijk}} dV$ refers to the volume of control cell Ω_{ijk} .

After space discretization performed by the central differences, we come up with a set of semi-discrete system of ordinary differential equations for each control cell Ω_{ijk}

$$\mathbf{P} \cdot \vec{W}_t|_{ijk}(t) = \mathbf{L}\vec{W}_{ijk}(t) + (\vec{f} + \vec{q})|_{ijk} \quad (31)$$

where $\mathbf{L}\vec{W}_{ijk}$ denotes the approximation of the right-hand side of (30) resulting from the space discretization

$$\mathbf{L}\vec{W}_{ijk} = -\frac{1}{\mu_{ijk}} \sum_{l=1}^6 [(\vec{F}_l - \vec{R}_l) \Delta S_1^l + (\vec{G}_l - \vec{S}_l) \Delta S_2^l + (\vec{H}_l - \vec{T}_l) \Delta S_3^l] \quad (32)$$

where all symbols denoted with subscript l refer to the l^{th} cell face of Ω_{ijk} and $(\Delta S_1^l, \Delta S_2^l, \Delta S_3^l)$ represents the l^{th} outer normal vector to the corresponding face of hexahedral control cell Ω_{ijk} .

Discretization of the inviscid numerical fluxes

The inviscid numerical fluxes $\vec{F}_l, \vec{G}_l, \vec{H}_l$ through the l -th face of Ω_{ijk} are computed as an average from the mean value over cell Ω_{ijk} and the mean value over the neighbor cell sharing the l -th face with cell Ω_{ijk} . Thus we get

$$\vec{F}_l = \frac{1}{2}(\vec{F}|_{\Omega_{ijk}} + \vec{F}|_{l\text{-th neighbor of } \Omega_{ijk}}),$$

$$\begin{aligned}\tilde{G}_l &= \frac{1}{2}(\vec{G}|_{\Omega_{ijk}} + \vec{G}|_{l\text{-th neighbor of } \Omega_{ijk}}), \\ \tilde{H}_l &= \frac{1}{2}(\vec{H}|_{\Omega_{ijk}} + \vec{H}|_{l\text{-th neighbor of } \Omega_{ijk}}) \quad l = 1, \dots, 6.\end{aligned}\quad (33)$$

Discretization of the viscous numerical fluxes

To compute the viscous fluxes at the l -th face of cell Ω_{ijk} , one has to know the derivatives of the velocity components at all six faces of each hexahedral control cell. The derivatives are evaluated using the dual control volumes of an octahedral shape denoted by $\bar{\Omega}_{ijk}^{(l)}$ as shown in the figure 1.

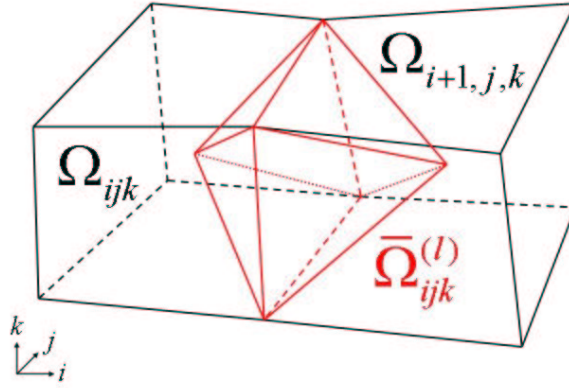


Fig. 1: A sketch of a dual control volume $\bar{\Omega}_{ijk}^{(l)}$ related to l -th face of Ω_{ijk} .

Four vertexes of the l -th face of cell Ω_{ijk} together with the center of Ω_{ijk} and the center of the l -th neighbor of cell Ω_{ijk} form the six vertexes of the dual control cell $\bar{\Omega}_{ijk}^{(l)}$ which is composed of eight dual faces. Hence, to compute *e.g.* the x -derivative of the u -velocity component at the l -th face of cell Ω_{ijk} we find by application of the “Mean value theorem” and the “Divergence theorem”

$$u_x|_{ijk}^{(l)} = \frac{1}{\bar{\mu}_{ijk}^{(l)}} \sum_{q=1}^8 \tilde{u}_q^{(l)} \Delta \bar{S}_1^{(l,q)} \quad l = 1, \dots, 6.\quad (34)$$

where $\bar{\mu}_{ijk}^{(l)} = \iiint_{\bar{\Omega}_{ijk}^{(l)}} d\bar{V}$ denotes the volume of the dual cell and the index q goes through all faces of the dual octahedral control volume and

$\Delta S_1^{(l,q)}$ abbreviates the the first component of the q -th outer normal vector related to the q -th face of the dual cell $\bar{\Omega}_{ijk}^{(l)}$. In a similar way, it is possible to compute the other derivatives of u , v and w components.

3.3 Time integration method

Let's remember the system of ordinary differential equations (31) resulting from the space discretization

$$\mathbf{P} \cdot \vec{W}_t|_{ijk}(t) = \mathbf{L}\vec{W}_{ijk}(t) + (\vec{f} + \vec{q})|_{ijk} \quad (35)$$

where \vec{W} represents the vector of computed quantities given by (26) which is related to the (S1)-system or by (27) concerning the (S2)-system. The system of ODEs (35) is integrated by the explicit 3-stage Runge-Kutta method hereafter rewritten as follows

$$\begin{aligned} \vec{W}_{ijk}^{(0)} &= \vec{W}_{ijk}^n \\ \vec{W}_{ijk}^{(m+1)} &= \vec{W}_{ijk}^{(0)} + \alpha_k \Delta t \left[\mathbf{B}\vec{W}_{ijk}^{(m)} + (\vec{f} + \vec{q})|_{ijk}^{(m)} \right], \quad m = 0, \dots, 2 \\ \vec{W}_{ijk}^{n+1} &= \vec{W}_{ijk}^{(3)} \end{aligned} \quad (36)$$

where $\alpha_0 = \frac{1}{2}$, $\alpha_1 = \frac{1}{2}$, $\alpha_2 = 1$ and the operator \mathbf{B} is defined by

$$\mathbf{B}\vec{W}_{ijk}^{(m)} = \mathbf{L}\vec{W}_{ijk}^{(m)} + \mathbf{D}\vec{W}_{ijk}^{(0)} \quad (37)$$

where \mathbf{L} refers to the space discretization operator (32) and \mathbf{D} represents the artificial diffusion term, see the next subsection.

Due to the explicit numerical formulation the stability limit criterion valid for a regular orthogonal meshes is applied, Kozel & Dvořák (1996) [4]

$$\Delta t \leq \min_{\Omega_{ijk}} \frac{CFL}{\frac{\varrho_A}{\Delta x} + \frac{\varrho_B}{\Delta y} + \frac{\varrho_C}{\Delta z} + 2 \cdot K \left(\frac{1}{\Delta x^2} + \frac{1}{\Delta y^2} + \frac{1}{\Delta z^2} \right)} \quad (38)$$

where ϱ_A , ϱ_B , ϱ_C refer to the spectral radii of the inviscid Jacobi's matrices, $CFL = 2$, K denotes the diffusion coefficient given by (3) and the rate of convergence to the steady state is examined component-wise using the residual norm

$$\|\mathbf{Rez} \vec{W}^n\|^2 = \left[\sum_{i,j,k} \left(\mathbf{B}\vec{W}_{ijk}^n + (\vec{f} + \vec{q})|_{ijk}^n \right)^2 \mu_{ijk} \right] / |\Omega|. \quad (39)$$

where $|\Omega|$ is volume of the computational domain.

3.4 The artificial diffusion

There are a few variants of the artificial diffusion term that can be adopted either of fourth or second order.

- In the first case, the fourth order artificial diffusion reads (in 1D)

$$\mathbf{D}^{(4)}\vec{W}_i^n = -\varepsilon^{(4)} \Delta x^4 \frac{\partial^4 \vec{W}}{\partial x^4} \quad (40)$$

and after discretization

$$\mathbf{D}^{(4)}\vec{W}_i^n = -\varepsilon^{(4)}(\vec{W}_{i+2} - 4\vec{W}_{i+1} + 6\vec{W}_i - 4\vec{W}_{i-1} + \vec{W}_{i-2}) \quad (41)$$

where the coefficient $\varepsilon^{(4)} \in \mathfrak{R}^+$ must be experimentally tuned as well. This term is applied to provide a necessary background numerical diffusion for a better convergence, mainly for the velocity–pressure flow field.

- In the second case, we use the following form (in 1D)

$$\mathbf{D}^{(2)}\vec{W}_i^n = +\varepsilon^{(2)} \Delta x^3 \frac{\partial}{\partial x} \left(\left| \frac{\partial \vec{W}}{\partial x} \right| \frac{\partial \vec{W}}{\partial x} \right)_i^n \quad (42)$$

and after discretization we get

$$\mathbf{D}^{(2)}\vec{W}_i^n = +\varepsilon^{(2)} \left[|\vec{W}_{i+1}^n - \vec{W}_i^n| (\vec{W}_{i+1}^n - \vec{W}_i^n) - |\vec{W}_i^n - \vec{W}_{i-1}^n| (\vec{W}_i^n - \vec{W}_{i-1}^n) \right] \quad (43)$$

where the coefficient $\varepsilon^{(2)} \in \mathfrak{R}^+$ has to be found experimentally as small as possible. Notice that $|\vec{W}|$ is applied component–wise and that in the 3D–case the procedure must be repeated also in the y and z –directions of coordinate system. This type of the artificial diffusion is used only during the solution of the transport equation for passive pollutant.

4 Validation

A detailed validation study has been performed on the systems (S1), (S2) in order to estimate the degree to which the models are an accurate representations of the real world from the perspective of their intended uses.

The chosen test case is based on a fully developed channel flow over a 2D polynomial-shaped hill mounted on a flat plate with a fairly large recirculation region in its wake. This test-case was considered at the 4th Workshop, organized by the University of Karlsruhe, IFH, April 1995 and now it is available in the ERCOFTAC's database. It consists of

- the experimental data due to Almeida (1993) [5]
- the reference numerical data received by the $k - \varepsilon$ turbulence model Davroux (1995) [6].

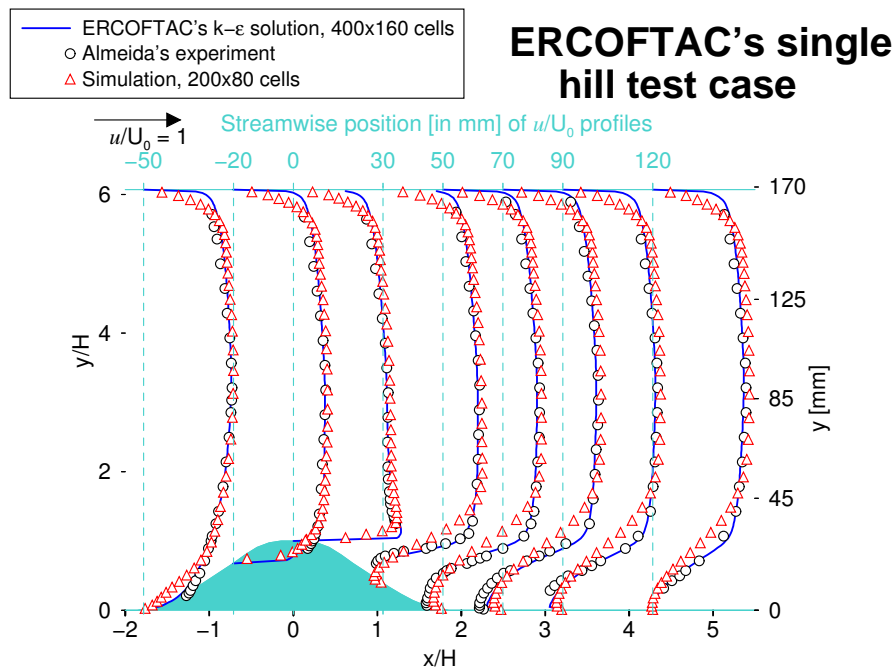


Fig. 2: Profiles of the u -velocity component normalized by U_0 , validation of (S1)-system with algebraic turbulence model.

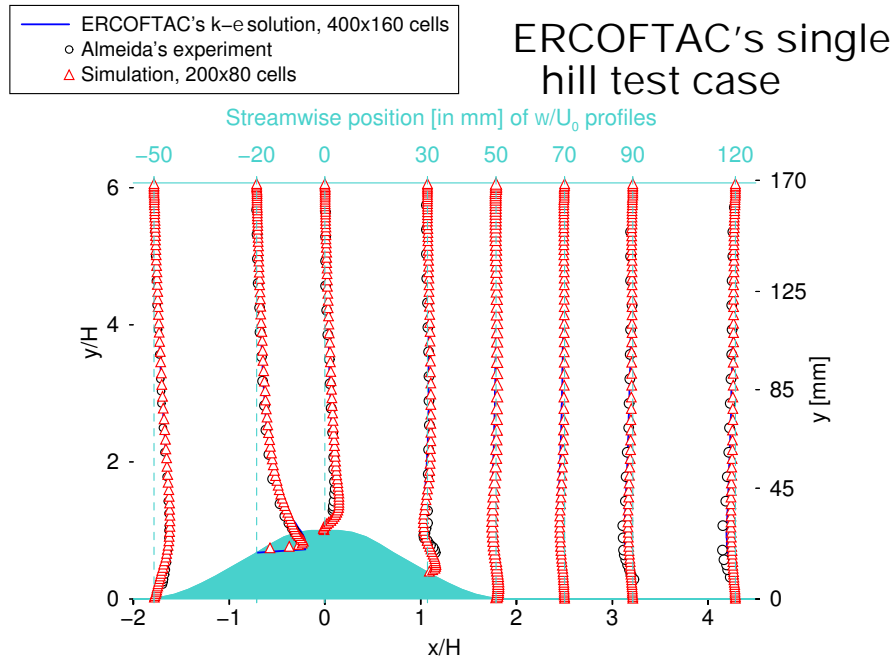


Fig. 3: Profiles of the w -velocity component normalized by U_0 , validation of (S1)-system with algebraic turbulence model

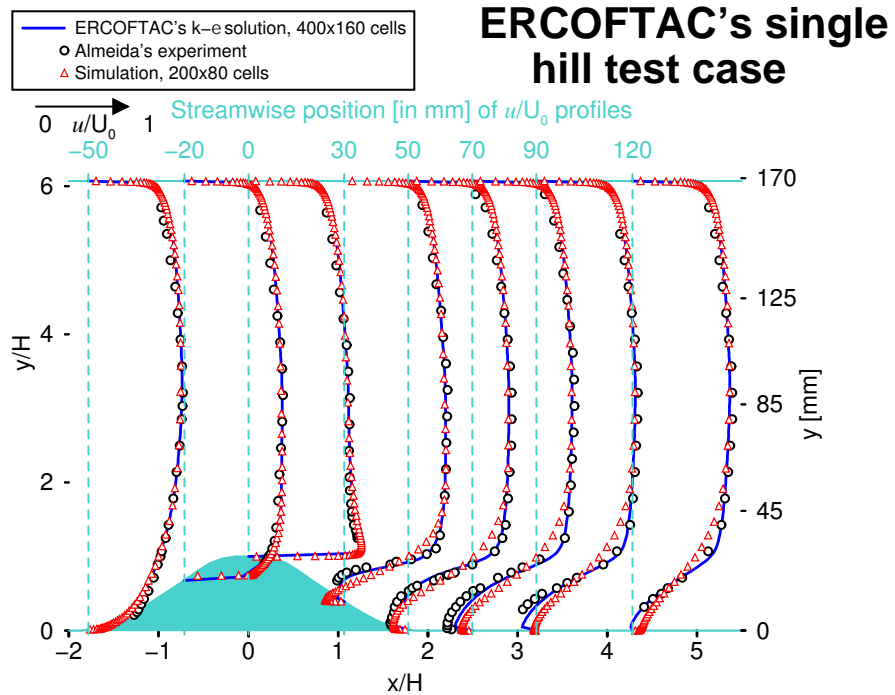


Fig. 4: Profiles of the u -velocity component normalized by U_0 , validation of (S2)-system with $k - \epsilon$ turbulence model.

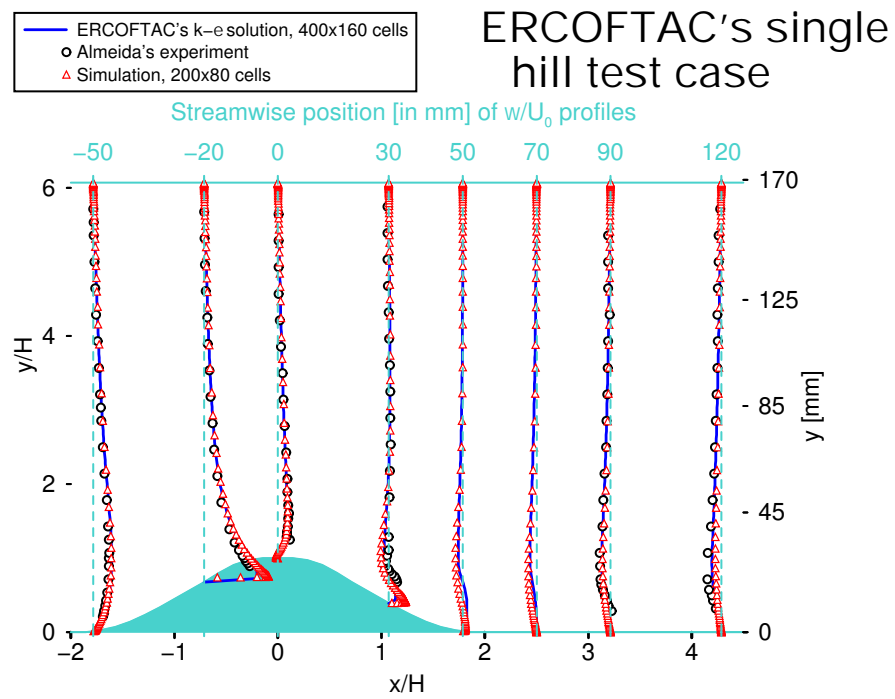


Fig. 5: Profiles of the w -velocity component normalized by U_0 , validation of (S2)-system with $k - \varepsilon$ turbulence model.

The results are summarized in section 6.

5 Applications

The system (S1) together with the numerical method is practically used to a few real–case 2D and 3D applications and moreover, some of the results are compared with the reference numerical data obtained by T. Bodnár (2004) [7] who has implemented a different mathematical model based on the Boussinesq approximation of the atmospheric boundary layer and the semi–implicit numerical method.

- The first set of results concerns with the 3D simulations over the Prague’s agglomeration with two different wall–modelling approaches: the no–slip and the wall–function concept, both of them compared.

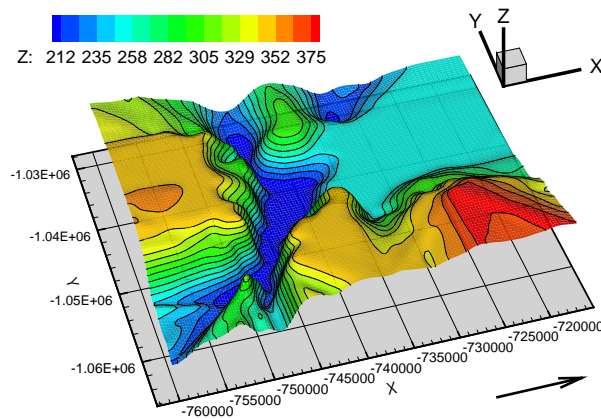


Fig. 6: The relief of Prague’s area colored by geographical altitude $[m]$.

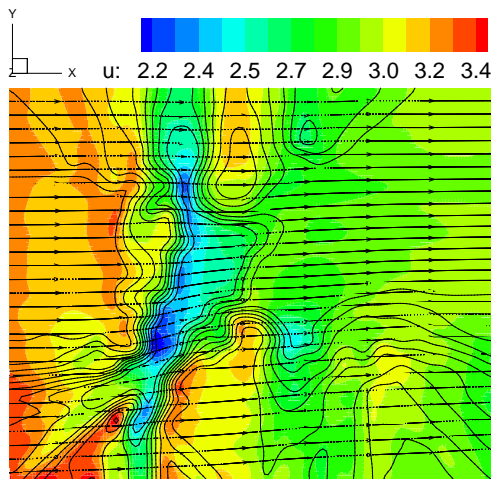


Fig. 7: Wall function.

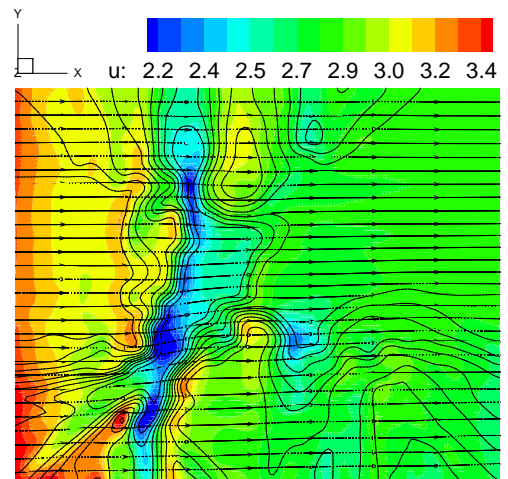


Fig. 8: No–slip wall.

The figures 7, 8 show the near-ground distribution of the u -velocity component [m/s] together with streamlines and geographical contours. One can see the overall not only qualitative agreement between the above two figures and also the effect of the Prague's valley which decelerates the flow and slightly deviates it from the original direction in the wall vicinity.

- The second collection of results is related to a 2D flow including a pollution dispersion over a complex coal field located in the North Bohemia which is also partially covered by a high forest stand in order to decelerate the flow locally and to decrease the level of downstream concentration of passive pollutant.

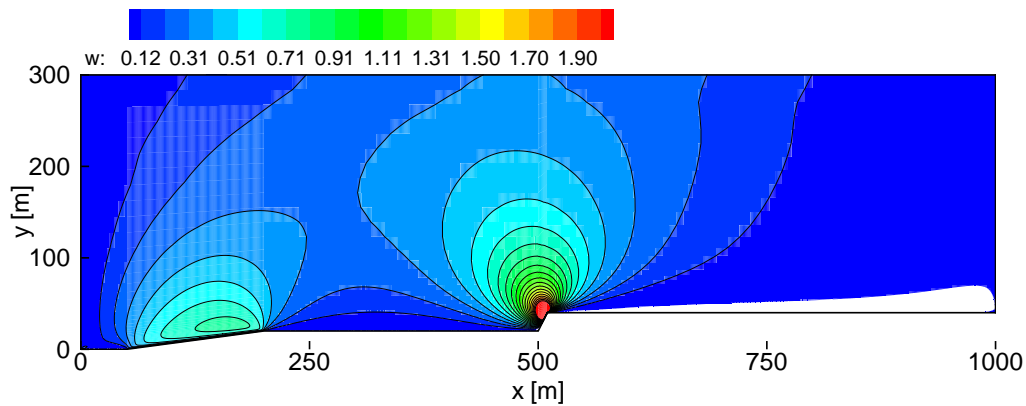


Fig. 9: Distrib. of the w -component [m/s], no forest.

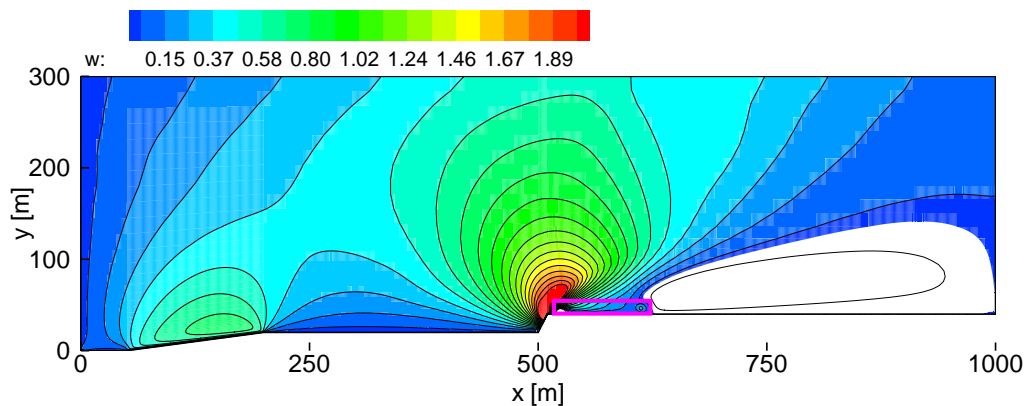


Fig. 10: Distrib. of the w -component [m/s], forest 15 m high, outlined by a pink rectangle.

The flow over the surface coal field is significantly influenced by the

presence of a forest. It also strongly depends on the forest dimensions and mainly on its drag coefficient. Practically in all computed cases, the flow is separated in the corner below the sudden step and a fairly large separation zone occurs in the presence of a forest stand of 15 m high where the bubble develops on the lee-side of the forest.

6 Summary

- VALIDATION: A practical results of this work can be found in the section related to a validation of (S1) and (S2) mathematical models. Even if the Reynolds number is several orders of magnitude lower than in a real atmosphere, the problem is still quite complex since a large separation zone develops behind a hill.

The algebraic model (modified for the channel flow using the Baldwin–Lomax model) has shown to give much better predictions for the length of separation zone: $4.3H$ in simulation compared to $4.4H$ in experiment normalized by the hill height H . On the other hand, the micro-scale version of the two-equation $k - \varepsilon$ model predicted length of zone $3.3H$ only. Therefore, this two-equation model is suitable for ABL problems without separation.

- WALL MODELLING: Two different applications have been defined and computed both with an ABL algebraic turbulence model:

- 1) The first one related to a 3D-flow over the Prague’s topography where a two different wall modelling strategies have been evaluated and compared. The first one is a classical no-slip wall modelling while the second one is based on concept of a wall-function for the velocity. The advantage of the first approach is its generality, however which is balanced by the use of a sufficiently fine grids in the wall region. The advantage of the second way of wall modelling lies in the fact that the computed profiles can be patched to some universal analytical profiles within the near-ground layer. Thus, the grids can be coarser in the vicinity of a wall. This leads to significant savings in CPU time. Notice, the flow should not be strongly influenced by a separation and this is the case of flow over the Prague’s area.

- FOREST MODELLING & POLLUTANT DISPERSION: The second case is related to a 2D-flow over a complex coal field including a pollution dispersion from an area source of pollutant (coal dust). As a special feature, a model for a high forest stand as a vegetation obstacle has been successfully implemented and the results have been compared to the other numerical results received by different numerical/mathematical model implemented by T. Bodnár. A quite acceptable agreement has been established for the flow over the forest stand for both methods.

Also it has been shown, the location of the forest stand as a shelter belt behind a source of pollutant can help to decrease the level of concentrations in the downstream region which is supposed to be inhabited. These simulations have been done together with cooperation of the Brown Coal Research Institute in Most.

- CLOSURE: The presented mathematical model is suitable to be used for a prediction of the velocity–pressure flow field and also passive pollutant dispersion over a complex topography. The numerical method has shown to be easy to implement and robust enough for a variety of ABL 2D and 3D simulations.

Reference

- [1] Jaňour Z.: Modelování mezní vrstvy atmosféry, Učební texty Karlovy University, Praha, 2001.
- [2] Blackadar A. K.: The vertical distribution of wind and turbulent exchange in a neutral atmosphere, *Journal Geoph. Research*, 67, 1962.
- [3] Speziale Ch. G., Abid R., Anderson E. C.: Critical Evaluation of two-equation models for near-wall turbulence, *AIAA Journal*, Vol. 30, pp. 324–331, 1992.
- [4] Kozel K., Dvořák R.: Matematické modelování v aerodynamice, skriptum FSI ČVUT, Praha, 1996.
- [5] Almeida G.P., Durao D.F.G., Heitor M.V.: Wake Flows Behind Two Dimensional Model Hills, *Exp. Thermal and Fluid Science*, 7, pp. 87, 1992.
- [6] Davroux A., Hoa C., Laurence D.: Flow Over a 2D Hill – Reference Solutions for k - ε and Second Moment Closure Turbulence Models, Workshop, Karlsruhe, 1995.
- [7] Beneš L., Bodnár T., Kozel K., Sládek I.: A Mathematical Study of the Vegetation Influence on the Atmospheric Flow over Complex Topography, In: “Topical Problems in Fluid mechanics 2004”, Praha, Ústav termomechaniky AV ČR, pp. 9–12, ISBN 80-85918-86-2.